PRAMANA
—journal of
physics



Vol. 50, No. 5,
May 1998
pp. 419–432

# Laser optogalvanic spectroscopy of argon in the wavelength region 605–740 nm

R C SHARMA, T KUNDU* and S N THAKUR
Laser Spectroscopy Laboratory, Physics Department, Banaras Hindu University, Varanasi 221 005, India
* Department of Physics, Indian Institute of Technology, Mumbai 400 076, India

MS received 5 November 1996; revised 23 January 1998

**Abstract.** Two-photon optogalvanic transitions in Ar glow discharge with Nd : YAG laser pumped dye laser excitation in the frequency range 13520–16520 $cm^{-1}$ has been studied using linear and circular polarization. The intensities of two-photon optogalvanic transitions are very sensitive to changes in the incident laser power which is not the case with one-photon transitions. Intensity ratio for circular and linear polarized light for two photon transitions $6s'[1/2]^\circ 1 \leftarrow 4s[3/2]^\circ 2$, $6s'[1/2]^\circ 0 \leftarrow 4s[3/2]^\circ 2$, and $5d[1/2]^\circ 0 \leftarrow 4s[3/2]^\circ 2, 5d[1/2]^\circ 1 \leftarrow 4s[3/2]^\circ 2$ are quite different from the other two-photon transitions. This has been explained as due to near one photon resonance of $4p'[3/2]1$ level for the first pair and $4p'[1/2]1$ for the second pair of transitions. The ratio of optogalvanic intensity for circular to linear polarized light has been theoretically estimated and compared with the observed results.

**Keywords.** Optogalvanic spectrum; two-photon transitions; laser spectroscopy.

**PACS Nos 52.80; 42.60**

## 1. Introduction

Optogalvanic spectroscopy of glow discharges is based on the detection of small changes in the plasma-impedance, with high signal to noise ratio. This change of impedance is caused by resonant absorption of monochromatic radiation from the tunable laser, by atomic or molecular species in the plasma. Hollow cathode discharges have been found particularly suitable for such studies on the excited electronic states and rare gas filled commercial hollow cathode lamps have also been used for the wavelength calibration of dye lasers [1–3]. Extensive studies of neon optogalvanic spectra have led to a great deal of information on its one-photon and two-photon transitions [2, 3]. In contrast, there are no reports on the two-photon optogalvanic transitions in argon in spite of several studies of its one-photon optogalvanic spectra [4–7]. There are also no systematic investigations of the extreme red end of the Ar optogalvanic spectrum apart from identification of about ten one-photon lines spread over the 695–795 nm region [4]. We report here, for the first time, two-photon optogalvanic transitions in Ar with Nd : YAG laser pumped dye laser excitation in the wavelength transitions region 605–740 nm (16520–13520 $cm^{-1}$). The one-photon excited optogalvanic transitions in this region are also included, many of them for the first time, in view of their importance as calibration standards.

## 2. Experimental

Frequency doubled output at 532 nm from the injection seeded continuum Nd : YAG laser (model YG681C) pumped a Lambda Physik dye laser (model LPD3002) at 10 Hz with energy per pulse 250 mJ. Three different laser dyes in methanol were used: LDS-730 (740–720 nm, region I), LDS-698 (720–670 nm, region II) and DCM (670–605 nm, region III). The spectral bandwidth of the dye laser was 0.2 $cm^{-1}$ with energies (at the peak of the dye laser output) per pulse (5 ns duration) of 35 mJ in region I, 70 mJ in region II and 45 mJ in region III. Approximately 20% of the dye laser radiation was coaxially directed into a Hamamatsu Ar-hollow cathode lamp (model L233-Fe) which was connected to a regular d.c. power supply (Keithley model 246) through a current limiting resistance of 2.5 k$\Omega$. The voltage across the lamp could be set between 180 and 200 volts for normal glow discharge and the optogalvanic voltage change of the discharge was monitored across a 2.5 k$\Omega$ resistance using a coupling capacitor of 5 $\mu$F. The laser beam spot was smaller than the cathode diameter of the lamp and the unfocused laser beam was carefully aligned so as not to fall on the metal surface. Our attempts to focus the laser beam (even weakly), in the glow discharge, led to pronounced instabilities in the optogalvanic signal.

The optogalvanic signal were monitored on an oscilloscope (Tektronix model 2465A) and simultaneously processed by a boxcar averager (model SR250); both units were

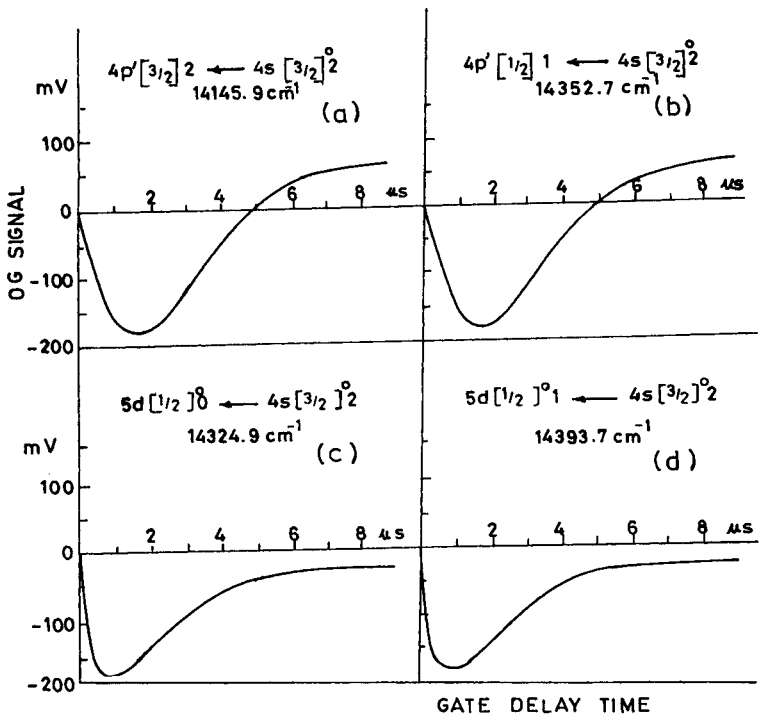


**Figure 1.** Oscilloscope traces of optogalvanic signals in argon corresponding to composite negative and positive voltage profiles (**a** and **b**) and only negative voltage profiles (**c** and **d**).

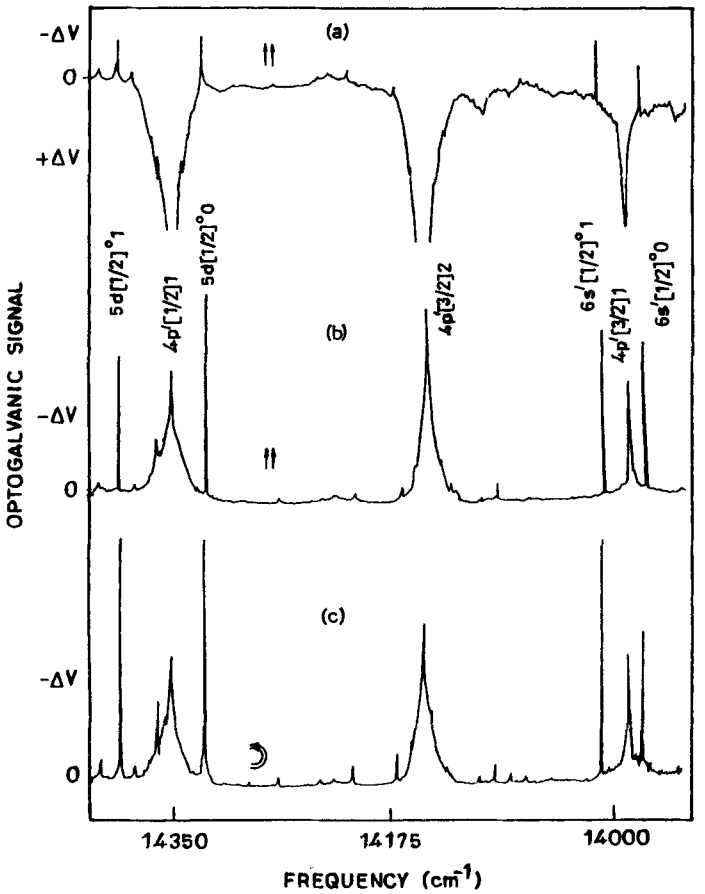


**Figure 2.** Optogalvanic spectra of Ar with a boxcar gate delay of (**a**) 13 μs (linear polarization) (**b**) 2 μs (linear polarization) and (**c**) 2 μs (circular polarization).

triggered by a photodiode receiving a small fraction of the incident dye laser pulse. A general survey of the temporal profile of the signals at several wavelengths showed that they could be grouped into two types as shown in oscilloscope traces in figure 1. The first group of transitions exhibit a negative voltage profile with a minimum at 1 μs from the excitation laser pulse and asymptotically increase to 0 after about 20 μs (figure 1c, d). The second group of optogalvanic transitions exhibit a composite voltage profile which starts with the negative voltage signal, becomes minimum after 2 μs then increases to a maximum positive voltage after 10 to 15 μs and asymptotically decreases to 0 at the end of 50 μs (figure 1a, b). The boxcar processed optogalvanic signals were recorded on a chart recorder with the dye laser grating scan rate of -0.3 nm/min. Figure 2 shows the optogalvanic spectra in the frequency region 13950–14400 $cm^{-1}$ (717–694 nm) recorded with the boxcar gate width of 2 μs and two different gate delays from the exciting laser pulse of 2 μs and 13 μs. It is seen from figure 2a (gate delay 13 μs) and figure 2b (gate delay 2 μs) that the relative negative voltage signal for the first group of optogalvanic

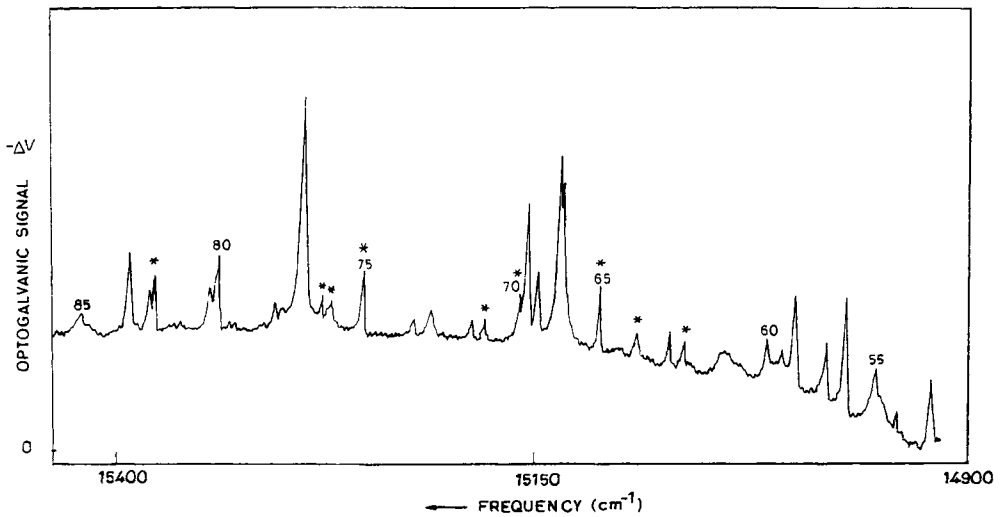


**Figure 3.** Optogalvanic spectrum of argon with a boxcar gate delay of 4 μs (linear polarization). The numbers within brackets correspond to serial number of transitions as in table 1 and (*) denote two-photon lines.

transitions are greatly diminished for the longer boxcar delay (figure 2a) and the optogalvanic signals for the second group become positive in polarity. It was found that the maximum number of Ar lines (all with the negative voltage signals) in any dye laser region were simultaneously recorded by setting the boxcar gate delay between 2 μs and 4 μs. The spectrum shown in figure 3 in the frequency region 14900–15400 $cm^{-1}$ (650–670 nm) is a part of the optogalvanic spectra in the DCM dye region (region III) recorded with the gate delay of 4 μs.

## 3. Spectroscopic assignments

The frequencies of the observed spectral lines were determined by fitting a second degree polynomial to the measured line positions with a maximum uncertainty of 1 $cm^{-1}$, these are given in the first column of table 1. The relative optogalvanic intensities (estimated from peak height for linearly polarized light) are given in the second column but these are not normalized for the spectral power variations of the dye laser output and in the case of overlapping transitions the relative intensities in the two dye regions are also shown (within bracket). The upper and lower energy levels of the transition, in Racah notation [8], are given in the third and fourth columns respectively and the transition type (one or two-photon) is shown in the fifth column. In region II, the relative intensities of two-photon transitions were also determined for circularly polarized light and the ratio ($\Omega$) of circular to linear polarization intensities is included in the fifth column along with the corresponding uncertainty. The spectroscopic assignments are quite straight forward in terms of the known energy levels of argon [9] and all, except ten of 142, observed lines have been satisfactorily assigned (see table 1). Some of the observed lines have two assignments within the limits of uncertainty.

**Table 1.** Observed one and two-photon optogalvanic transition in argon in the wavelength region 605–740 nm (16516–13520 $cm^{-1}$).

| Frequency ($cm^{-1}$) | Relative intensity | Assignment | | Transition type ($\Omega$) |
|---|---|---|---|---|
| | | Upper state | Lower state | |
| Region I (Dye LDS-730) | | | | |
| 13523.2 | 03 | $6s[3/2]^\circ 1$ | $4p[3/2]2$ | OP |
| 13539.9 | 18 | $4p'[3/2]2$ | $4s[3/2]^\circ 1$ | OP |
| | | $7s[3/2]^\circ 1$ | $4s'[1/2]^\circ 1$ | TP |
| 13561.4 | 10 | $4d[7/2]^\circ 4$ | $4p[5/2]3$ | OP |
| 13595.3 | 12 | $4d[7/2]^\circ 3$ | $4p[5/2]2$ | OP |
| 13610.5 | 04 | $4d[3/2]^\circ 1$ | $4p[3/2]2$ | OP |
| 13664.8 | 07 | $6s'[1/2]^\circ 1$ | $4p'[1/2]1$ | OP |
| 13673.2 | 04 | $6s[3/2]^\circ 1$ | $4p[3/2]1$ | OP |
| 13705.4 | 14 | $6s'[1/2]^\circ 1$ | $4s[3/2]^\circ 1$ | TP |
| 13722.1 | 05 | $4d'[3/2]^\circ 1$ | $4p'[3/2]2$ | OP |
| 13745.8 | 35 | $4p'[1/2]^\circ 1$ | $4s[3/2]^\circ 1$ | OP |
| 13749.9 | 17 | $4d[7/2]^\circ 3$ | $4p[5/2]3$ | OP |
| 13757.1 | 03 | $7s[3/2]^\circ 1$ | $4p'[1/2]0$ | OP |
| 13760.5 | 05 | $4d[3/2]^\circ 1$ | $4p[3/2]1$ | OP |
| 13804.9 | 06 | $4d'[5/2]^\circ 3$ | $4s[3/2]^\circ 2$ | TP |
| 13827.5 | 09 | $4d[5/2]^\circ 2$ | $4p[5/2]2$ | OP |
| 13872.0 | 17(b) | $6s'[1/2]^\circ 1$ | $4p'[3/2]2$ | OP |
| 13880.0 | 05 | $4d'[3/2]^\circ 1$ | $4p'[3/2]1$ | OP |
| 13930.0 | 05(b) | — | unassigned | |
| 13944.4 | 05 | $7s[3/2]^\circ 2$ | $4s'[1/2]^\circ 0$ | TP |
| 13948.3 | 07 | $4d[5/2]^\circ 3$ | $4p[5/2]2$ | OP |
| Region II (Dye-LDS-698) | | | | |
| 13976.6 | 70 | $6s'[1/2]^\circ 0$ | $4s[3/2]^\circ 2$ | TP ($0.9 \pm 0.1$) |
| 13988.3 | 60 | $4p'[3/2]1$ | $4s[3/2]^\circ 2$ | OP |
| 14008.8 | 80 | $6s'[1/2]^\circ 1$ | $4s[3/2]^\circ 2$ | TP ($1.3 \pm 0.1$) |
| 14079.2 | 06 | $5d'[5/2]^\circ 3$ | $4s'[1/2]^\circ 1$ | TP ($2.0 \pm 0.1$) |
| 14091.6 | 11 | $5d[1/2]^\circ 1$ | $4s[3/2]^\circ 1$ | TP ($0.7 \pm 0.2$) |
| 14104.3 | 04 | $4d[5/2]^\circ 3$ | $4p[5/2]3$ | OP |
| 14128.2 | 06 | | unassigned | |
| 14145.9 | 100 | $4p'[3/2]2$ | $4s[3/2]^\circ 2$ | OP |
| 14168.4 | 07 | $5d[3/2]^\circ 2$ | $4s[3/2]^\circ 1$ | TP ($2.1 \pm 0.2$) |
| 14204.5 | 06 | $5d[7/2]^\circ 3$ | $4s[3/2]^\circ 1$ | TP ($1.9 \pm 0.2$) |
| 14222.3 | 03 | $4d[5/2]^\circ 3$ | $4p[5/2]3$ | OP |
| 14231.8 | 02 | $4d[3/2]^\circ 1$ | $4p[5/2]2$ | OP |
| 14266.5 | 04 | $5d[5/2]^\circ 2$ | $4s[3/2]^\circ 1$ | TP ($2.1 \pm 0.1$) |
| 14290.5 | 02 | $5d'[5/2]^\circ 3$ | $4s[3/2]^\circ 1$ | TP ($2.0 \pm 0.1$) |
| 14297.8 | 02 | $6s[3/2]^\circ 1$ | $4p[5/2]3$ | OP |

(*Continued*)

**Table 1.** (*Continued*)

| Frequency ($cm^{-1}$) | Relative intensity | Assignment | | Transition type ($\Omega$) |
|---|---|---|---|---|
| | | Upper state | Lower state | |
| 14324.9 | 100 | $5d[1/2]°0$ | $4s[3/2]°2$ | TP ($1.1 \pm 0.1$) |
| 14352.7 | 65 | $4p'[1/2]1$ | $4s[3/2]°2$ | OP |
| 14365.0 | 15 | $7s[3/2]°1$ | $4s[3/2]°1$ | TP ($0.9 \pm 0.2$) |
| 14382.0 | 06 | $5d[3/2]°1$ | $4s[3/2]°1$ | TP ($0.8 \pm 0.2$) |
| 14393.7 | 65 | $5d[1/2]°1$ | $4s[3/2]°2$ | TP ($1.5 \pm 0.1$) |
| 14410.0 | 07 | $5d'[3/2]°2$ | $4s'[1/2]°0$ | TP ($2.0 \pm 0.2$) |
| 14445.9 | 13 | $5d[7/2]°4$ | $4s[3/2]°2$ | TP ($2.1 \pm 0.2$) |
| 14471.7 | 20 | $5d[3/2]°2$ | $4s[3/2]°2$ | TP ($0.7 \pm 0.2$) |
| 14475.7 | 05 | $5d'[5/2]°2$ | $4s'[1/2]°0$ | TP ($1.9 \pm 0.2$) |
| 14508.7 | 03 | $5d[7/2]°3$ | $4s[3/2]°2$ | TP ($2.0 \pm 0.2$) |
| 14515.3 | | | (unassigned) | |
| 14550.5 | 03 | $4d[1/2]°1$ | $4p[1/2]1$ | OP |
| 14592.8 | 15 | $5d[3/2]°2$ | $4p'[1/2]1$ | OP |
| 14592.8 | 04 | $5d[5/2]°3$ | $4s[3/2]°2$ | TP ($2.0 \pm 0.2$) |
| 14648.7 | 09 | $7s[3/2]°2$ | $4s[3/2]°2$ | TP ($0.7 \pm 0.2$) |
| 14785.7 | 10 | $5d[5/2]°2$ | $4p'[1/2]1$ | OP |
| 14803.1 | | | (unassigned) | |
| Region III (Dye-DCM) | | | | |
| 14924.5 | 25 | $4d'[3/2]°1$ | $4p[3/2]1$ | OP |
| | | $6s'[1/2]°1$ | $4p[3/2]2$ | OP |
| 14944.5 | 08 | $7s[3/2]°2$ | $4p'[1/2]1$ | OP |
| 14956.2 | 20 | $5d[3/2]°2$ | $4p'[3/2]1$ | OP |
| 14972.5 | 40 | $4p'[1/2]0$ | $4s[3/2]°1$ | OP |
| 14983.5 | 18 | $4d'[3/2]°2$ | $4p[5/2]2$ | OP |
| | | $7s[3/2]°1$ | $4p'[1/2]1$ | OP |
| 15002.0 | 35 | $4d'[5/2]°2$ | $4p[5/2]2$ | OP** |
| 15010.1 | 04 | $6s'[1/2]°0$ | $4p[3/2]1$ | OP |
| 15018.1 | 08 | $5d[3/2]°1$ | $4p'[1/2]1$ | OP |
| 15039.7 | 10 (b) | $5d[5/2]°3$ | $4p'[3/2]2$ | OP |
| 15065.5 | 09 | $7s'[1/2]°1$ | $4s[3/2]°1$ | TP |
| 15074.7 | 09 | $6s'[1/2]°1$ | $4p[3/2]1$ | OP |
| 15093.2 | 08 | $8s[3/2]°1$ | $4s[3/2]°1$ | TP |
| 15114.5 | 30 | $5d'[3/2]°2$ | $4s[3/2]°2$ | TP |
| 15136.2 | 70 | $4d'[5/2]°3$ | $4p[5/2]2$ | OP |
| 15137.8 | 75 | $4d'[3/2]°2$ | $4p[5/2]3$ | OP |
| 15150.2 | 28 | $4d[5/2]°2$ | $4p'[3/2]1$ | OP |
| 15155.7 | 60 | $4d'[5/2]°2$ | $4p[5/2]3$ | OP** |
| 15161.2 | 06 | $6d[1/2]°1$ | $4s[3/2]°2$ | TP |
| 15181.8 | 06 | $6d[1/2]°0$ | $4s[3/2]°2$ | TP |
| 15190.1 | 06 | $7s[3/2]°1$ | $4p'[3/2]2$ | OP |

(*Continued*)

**Table 1.** (*Continued*)

| Frequency ($cm^{-1}$) | Relative intensity | Assignment | | Transition type ($\Omega$) |
|---|---|---|---|---|
| | | Upper state | Lower state | |
| 15213.7 | 09 | $8s[3/2]°1$ | $4p'[1/2]0$ | OP |
| 15224.8 | 06 | $5d[3/2]°1$ | $4p'[3/2]2$ | OP |
| 15254.0 | 20 | $6d[7/2]°4$ | $4s[3/2]°2$ | TP |
| 15273.6 | 07 | $10d[5/2]°2$ | $4s'[1/2]°1$ | TP |
| 15279.2 | 07 | $6d'[5/2]°2$ | $4s'[1/2]°0$ | TP |
| 15290.4 | 90 | $4d'[5/2]°3$ | $4p[5/2]3$ | OP** |
| 15308.1 | 07 | $7s[3/2]°2$ | $4p'[3/2]1$ | OP |
| 15342.2 | 25 | $4d[5/2]°2$ | $4p'[1/2]1$ | OP |
| 15347.0 | 12 | $7s[3/2]°2$ | $4p'[3/2]1$ | OP |
| 15379.1 | 14 | $8s[3/2]°2$ | $4s[3/2]°2$ | TP |
| 15382.5 | 12 | $5d[3/2]°1$ | $4p'[3/2]1$ | OP |
| 15394.4 | 28 | $4d'[3/2]°1$ | $4p[5/2]2$ | OP |
| 15426.1 | 05 | $7s[3/2]°1$ | $4p[1/2]0$ | OP |
| 15449.2 | 03 | $7d[7/2]°3$ | $4s[3/2]°1$ | TP |
| 15460.8 | 08 | $5d[3/2]°1$ | $4p[1/2]0$ | OP |
| 15491.7 | 03 (b) | | unassigned | |
| 15515.9 | 03 | $9s[3/2]°1$ | $4s[3/2]°1$ | TP |
| 15544.3 | 25 | $6s'[1/2]°1$ | $4p[5/2]2$ | OP |
| 15580.9 | 100 | $6s[3/2]°2$ | $4p[1/2]1$ | OP |
| 15624.8 | 02 (b) | | unassigned | |
| 15641.7 | 03 (b) | | unassigned | |
| 15657.3 | 75 | $6s[3/2]°1$ | $4p[1/2]1$ | OP |
| 15695.1 | 50 | $5d[1/2]°1$ | $4p[3/2]2$ | OP |
| 15706.4 | 30 | $5d[1/2]°0$ | $4p[3/2]1$ | OP |
| 15729.8 | 08 | $7d[3/2]°2$ | $4s[3/2]°2$ | TP |
| 15732.8 | 14 | $7d[7/2]°4$ | $4s[3/2]°2$ | TP |
| 15744.8 | 35 | $4d[3/2]°1$ | $4p[1/2]1$ | OP |
| 15785.1 | 03 | $7d[5/2]°3$ | $4s[3/2]°2$ | TP |
| 15790.2 | 03 | $10s[3/2]°1$ | $4s[3/2]°1$ | TP |
| 15813.6 | 13 | $9s[3/2]°2$ | $4s[3/2]°2$ | TP |
| 15832.6 | 07 | $7d[1/2]°1$ | $4p'[1/2]0$ | OP |
| 15845.6 | 50 | $5d[1/2]°1$ | $4p[3/2]1$ | OP |
| 15849.8 | 70 | $5d[3/2]°2$ | $4p[3/2]2$ | OP |
| 15877.0 | 25 | $5d'[3/2]°2$ | $4p'[1/2]1$ | OP |
| 15922.6 | 40 | $5d[7/2]°3$ | $4p[3/2]2$ | OP |
| 15961.7 | 04 | $6d'[7/2]°2$ | $4s[3/2]°2$ | TP |
| 15972.1 | 15 | $6d[1/2]°1$ | $4p'[1/2]1$ | OP |
| 16000.7 | 25 | $5d[3/2]°2$ | $4p[3/2]1$ | OP |
| 16009.9 | 12 | $8d[1/2]°0$ | $4s[3/2]°2$ | TP |
| 16013.0 | 12 | $6d[1/2]°0$ | $4p'[1/2]1$ | OP |
| 16037.7 | 06 | $8d[7/2]°4$ | $4s[3/2]°2$ | TP |

(*Continued*)

**Table 1.** (*Continued*)

| Frequency ($cm^{-1}$) | Relative intensity | Assignment | | Transition type ($\Omega$) |
|---|---|---|---|---|
| | | Upper state | Lower state | |
| 16045.4 | 35 | $5d[5/2]°2$ | $4p[3/2]2$ | OP |
| 16083.5 | 60 | $5d'[3/2]°2$ | $4p'[3/2]2$ | OP |
| 16092.9 | 75 | $5d[5/2]°3$ | $4p[3/2]2$ | OP |
| | | $10s[3/2]°2$ | $4s[3/2]°2$ | TP |
| 16127.2 | 03 | | unassigned | |
| 16165.5 | 25 (b) | | unassigned | |
| 16178.8 | 13 | $6d[1/2]°1$ | $4p'[3/2]2$ | OP |
| 16195.5 | 40 | $5d[5/2]°2$ | $4p[3/2]1$ | OP |
| 16202.7 | 55 | $7s[3/2]°2$ | $4p[3/2]2$ | OP |
| | | $11d[7/2]°3$ | $4s[3/2]°1$ | TP |
| 16216.4 | 40 | $5d'[5/2]°2$ | $4p'[3/2]2$ | OP |
| 16242.4 | 50 | $7s[3/2]°1$ | $4p[3/2]2$ | OP |
| 16267.8 | 30 | $5d'[5/2]°3$ | $4p'[3/2]2$ | OP |
| 16276.7 | 17 | $5d[3/2]°1$ | $4p[3/2]2$ | OP |
| 16312.3 | 14 | $6d[3/2]°2$ | $4p'[1/2]1$ | OP |
| 16315.5 | 28 | $5d[1/2]°1$ | $4p[5/2]2$ | OP |
| 16318.7 | 14 | $5d'[3/2]°1$ | $4p'[1/2]1$ | OP |
| 16329.9 | 13 | $6d[5/2]°2$ | $4p'[1/2]1$ | OP |
| 16336.3 | 14 | $6d[1/2]°1$ | $4p'[3/2]1$ | OP |
| 16353.1 | 13 | $7s[3/2]°1$ | $4p[3/2]1$ | OP |
| 16376.3 | 50 | $6d[1/2]°0$ | $4p'[3/2]1$ | OP |
| 16386.0 | 45 | $7s'[1/2]°1$ | $4p'[1/2]1$ | OP |
| 16391.2 | 40 | $7s[3/2]°1$ | $4p[3/2]1$ | OP |
| 16406.2 | 05 | $8s[3/2]°2$ | $4p'[1/2]1$ | OP |
| 16413.3 | 30 | $6d[1/2]°1$ | $4p[1/2]0$ | OP |
| 16426.2 | 10 | $5d[3/2]°1$ | $4p[3/2]1$ | OP |
| 16439.1 | 10 | $8s[3/2]°1$ | $4p'[1/2]1$ | OP** |
| 16453.0 | 15 (b) | | unassigned | |
| 16483.9 | 12 | $6d[7/2]°3$ | $4p'[3/2]2$ | OP |
| 16498.5 | 25 | $4d'[3/2]°2$ | $4p[1/2]1$ | OP** |
| 16516.0 | 18 | $4d'[5/2]°2$ | $4p[1/2]1$ | OP |

(b): Broad feature; **: Revised assignment from those in Ref [6].

The metastable $4s[3/2]°2$ level accounts for more than half of the 44 two-photon resonant transitions whereas 14 of them originate in $4s[3/2]°1$, four in $4s'[1/2]°0$ and only three in $4s'[1/2]°1$ level. A partial energy level diagram of argon is given in figure 4 to explain the origin of some very intense spectral lines. The intensities of two-photon optogalvanic transitions are very sensitive to changes in incident laser power, unlike the one photon transition. The strongest two-photon lines are observed at 13976.6, 14008.8, 14324.9 and 14393.7 $cm^{-1}$ respectively, all of them originating in

**Table 2.** Intensity ratio ($\Omega$) circular to linear polarized radiation of the two-photon transitions.

| Transition frequency ($cm^{-1}$) | Assignment | | Observed ($\Omega$) | Calculated ($\Omega$) |
|---|---|---|---|---|
| | Upper state | Lower state | | |
| 13976.6 | $6s'[1/2]^\circ 0$ | $4s[3/2]^\circ 2$ | $(0.9 \pm 0.1)$ | 1.5 |
| 14008.8 | $6s'[1/2]^\circ 1$ | $4s[3/2]^\circ 2$ | $(1.3 \pm 0.1)$ | 1.5 |
| 14079.2 | $5d'[5/2]^\circ 3$ | $4s'[1/2]^\circ 1$ | $(2.0 \pm 0.1)$ | 1.5 |
| 14091.6 | $5d[1/2]^\circ 1$ | $4s[3/2]^\circ 1$ | $(0.7 \pm 0.2)$ | 1.0 |
| 14168.4 | $5d[3/2]^\circ 2$ | $4s[3/2]^\circ 1$ | $(2.1 \pm 0.2)$ | 1.5 |
| 14204.5 | $5d[7/2]^\circ 3$ | $4s[3/2]^\circ 1$ | $(1.9 \pm 0.2)$ | 1.5 |
| 14266.5 | $5d[5/2]^\circ 2$ | $4s[3/2]^\circ 1$ | $(2.1 \pm 0.1)$ | 1.5 |
| 14290.5 | $5d'[5/2]^\circ 3$ | $4s[3/2]^\circ 1$ | $(2.0 \pm 0.1)$ | 1.5 |
| 14324.9 | $5d[1/2]^\circ 0$ | $4s[3/2]^\circ 2$ | $(1.1 \pm 0.1)$ | 1.5 |
| 14365.0 | $7s[3/2]^\circ 1$ | $4s[3/2]^\circ 1$ | $(0.9 \pm 0.2)$ | 1.0 |
| 14382.0 | $5d[3/2]^\circ 1$ | $4s[3/2]^\circ 1$ | $(0.8 \pm 0.2)$ | 1.0 |
| 14393.7 | $5d[1/2]^\circ 1$ | $4s[3/2]^\circ 2$ | $(1.5 \pm 0.1)$ | 1.5 |
| 14410.0 | $5d'[3/2]^\circ 2$ | $4s'[1/2]^\circ 0$ | $(2.0 \pm 0.2)$ | 1.5 |
| 14445.9 | $5d[7/2]^\circ 4$ | $4s[3/2]^\circ 2$ | $(2.1 \pm 0.2)$ | 1.5 |
| 14471.7 | $5d[3/2]^\circ 2$ | $4s[3/2]^\circ 2$ | $(0.7 \pm 0.2)$ | 0.6 |
| 14475.7 | $5d'[5/2]^\circ 2$ | $4s'[1/2]^\circ 0$ | $(1.9 \pm 0.2)$ | 1.5 |
| 14508.7 | $5d[7/2]^\circ 3$ | $4s[3/2]^\circ 2$ | $(2.0 \pm 0.2)$ | 1.5 |
| 14592.8 | $5d[5/2]^\circ 3$ | $4s[3/2]^\circ 2$ | $(2.0 \pm 0.2)$ | 1.5 |
| 14648.7 | $7s[3/2]^\circ 2$ | $4s[3/2]^\circ 2$ | $(0.7 \pm 0.2)$ | 0.6 |

the $4s[3/2]^\circ 2$ level. The relative intensities of these transitions under linear and circular polarizations are shown in figures 2b and 2c respectively and discussed in the next section.

Only ten of the one-photon transitions have been observed in the region II (table 1) of which three have metastable states as their lower energy levels. They originate in $4s[3/2]^\circ 2$ level and are very strong, probably power broadened due to high laser intensity (see figure 2). The transitions originating in $4p[5/2]2$, $4p[5/2]3$ and $4p[1/2]1$ give rise to weak optogalvanic signals. All the one-photon optogalvanic transitions in regions I and II and many of them in region III have been observed for the first time; for some of the transitions in region III reported earlier [6] we have noticed printing or assignment errors (marked ** in table 1).

## 4. Discussion and results

The lowest excited levels in Ar (electronic configuration $3p^5 4s$) in the order of increasing energy are : $4s[3/2]^\circ 2$, $4s[3/2]^\circ 1$, $4s[3/2]^\circ 0$, $4s'[1/2]^\circ 0$, $4s'[1/2]^\circ 1$ (see figure 4) of which the first three are primarily $^3P$ in character and the last one is $^1P$ in the L-S coupling scheme. $4s[3/2]^\circ 2$ and $4s'[1/2]^\circ 0$ are truly metastable states, whereas $4s[3/2]^\circ 1$ is not

quite so due to slight triplet-singlet mixing [10] and $4s'[1/2]^\circ 1$ has a dipole allowed transition to the ground state. The next set of excited energy levels arise from the $3p^5 4p$ configuration and decay primarily to the $4s$ and $4s'$ levels with a radiative life time in the range of 10–20 ns. Temporal profile of the optogalvanic voltage signal resulting from a transition between two excited states is given by [11]:

$$\Delta V = -V_0(n_1 - n_2)[a_2 \exp(-t/T_2) - a_1 \exp(-t/T_1)], \tag{1}$$

where $a_2$, $a_1 (a_2 > a_1)$ are characteristic phenomenological constants, $T_2$, $T_1$ the relaxation times and $n_2$, $n_1$ the atomic populations of the upper and lower energy levels respectively. $V_0$ is a constant for a particular transition and depends on its optical absorption cross section as well as the discharge and circuit parameters.

In temporal profile of the optogalvanic signals immediately after the laser excitation pulse ($t = 0$) the voltage is negative because of the dominance of the first term within the square brackets of eq. (1). This is exemplified by all the transitions shown in figure 2b. For the optogalvanic transitions with $4s[3/2]^\circ 2$ as the lower state and $4p'[3/2]2$, $4p'[3/2]1$, $4p'[1/2]1$ as upper states, the signals are positive for long time delay (figure 2a) but negative for short delay (figure 2b) after the exciting laser pulse. The composite negative and positive optogalvanic signals appear because of $T_2 < T_1$, so that the first term in eq. (1) dominates at short delays and the second term becomes more dominant for longer delays after the exciting laser pulse. This implies that the upper states of these transitions have relaxation times comparable to those of the lower states in accordance with eq. (1).

The observed ratio $\Omega$ of two-photon intensities with circular and linear polarization can be broadly grouped into two categories. For transitions with equal $J$ for the upper and lower states $\Omega \approx 0.7$ and for those with unequal $J$ values, it is close to 2. Four of the strongest two-photon lines, however, do not show this polarization behaviour (see table 1).

Grynberg *et al* [12] have carried out a detailed analysis of optogalvanic intensity, arising from the scalar and the quadrupolar components of the two-photon transition tensor for Doppler-free two-photon spectrum of neon. They conclude that the experimental observations on polarization characteristics do not agree with theoretical prediction unless one makes use of accurate wavefunctions for the initial, final and various intermediate states. We also qualitatively account for the observed ratio ($\Omega$) in the following way. We have calculated the optogalvanic intensity ratios of circular to linear polarized light ($\Omega =$ circular/linear) by evaluating the contributions of scalar and quadrupolar components using the two-photon matrix given by Grynberg *et al* [12];

$$\begin{aligned}\Gamma_g &= \frac{A}{2J_g+1} \sum_{k=0,2} \frac{|\langle eJ_e||Q^k||gJ_g\rangle|^2}{2k+1} \left(\sum |a_q^k(\varepsilon_1, \varepsilon_2)|^2\right) \\ &= \frac{A}{2J_g+1} \left[\frac{|\langle eJ_e||Q^0||gJ_g\rangle|^2}{1} (|a_0^0(\varepsilon_1, \varepsilon_2)|^2) \right. \\ &\qquad \left. + \frac{|\langle eJ_e||Q^2||gJ_g\rangle|^2}{5} \left(\sum_q |a_q^2(\varepsilon_1, \varepsilon_2)|^2\right)\right] \end{aligned} \tag{2}$$

where $\varepsilon_1$, $\varepsilon_2$ represent identical polarizations for the two-photons. Using

$$\left.\begin{aligned} |a_0^0(\varepsilon_1,\varepsilon_2)|^2 &= 1/3 \\ \sum |a_q^2(\varepsilon_1,\varepsilon_2)|^2 &= 2/3 \end{aligned}\right| \quad \text{for linear polarization,} \tag{3}$$

$$\left.\begin{aligned} |a_0^0(\varepsilon_1,\varepsilon_2)|^2 &= 0 \\ \sum |a_q^2(\varepsilon_1,\varepsilon_2)|^2 &= 1 \end{aligned}\right| \quad \text{for circular polarization,} \tag{4}$$

we get

$$\Gamma_{g(\text{circular})} = \frac{A}{2J_g+1}\left[\frac{|\langle eJ_e\|Q^2\|gJ_g\rangle|^2}{5}\right], \tag{5}$$

$$\Gamma_{g(\text{linear})} = \frac{A}{2J_g+1}\left[\frac{1}{3}\frac{|\langle eJ_e\|Q^0\|gJ_g\rangle|^2}{1} + \frac{2}{15}\frac{|\langle eJ_e\|Q^2\|gJ_g\rangle|^2}{1}\right] \tag{6}$$

and hence

$$\begin{aligned} \Omega &= \Gamma_{g(\text{circular})}/\Gamma_{g(\text{linear})} \\ &= \frac{1/5C}{1/3B + 2/15C}, \end{aligned} \tag{7}$$

where

$$B = |\langle eJ_e\|Q^0\|gJ_g\rangle|^2,$$
$$C = |\langle eJ_e\|Q^2\|gJ_g\rangle|^2.$$

The following derivations of $\Omega$ are valid only when there is only one intermediate real level with energy close to that of one photon.

*Case* 1. When $J_e$ is different from $J_g$, then $|\langle eJ\|Q^0\|gJ\rangle|^2 = 0$ so that

$$\Omega = \frac{1/5}{2/15} = 1.5. \tag{8}$$

*Case* 2. When $J_e$ is equal to $J_g$ and greater than or equal to 1, then

$$R = \frac{|\langle eJ_e\|Q^0\|gJ_g\rangle|^2}{1/5|\langle eJ_e\|Q^2\|gJ_g\rangle|^2} = \frac{B}{1/5C}, \tag{9}$$

where $R$ is the ratio of scalar to quadrupolar components, the value of $R$ has been calculated from the Racah coefficients according to the following relation:

$$R(g,e.J_r) = \frac{1}{3(2J_g+1)\begin{bmatrix} J_e & J_g & 2 \\ 1 & 1 & J_r \end{bmatrix}^2},$$
$$R = 1 \quad \text{if } J_e = J_g = 1; \quad R = 3 \quad \text{if } J_e = J_g = 2, \tag{10}$$

where $J_r$ is the angular momentum of the real intermediate level. Now from eqs (7) and

(9), $\Omega$ is given by

$$\Omega = \frac{1/5}{1/15R + 2/15},$$
$$\Omega = 1 \quad \text{if } R = 1; \quad \Omega = 0.6 \quad \text{if } R = 3. \tag{11}$$

The observed values of $\Omega$ for transitions at 14471.7 $cm^{-1}$ and 14648.7 $cm^{-1}$ as shown in table 2 are in good agreement with the calculated value of 0.6 corresponding to transitions between two levels with $J' = J'' = 2$. Similarly the observed values of $\Omega$ for transitions at 14365.0 $cm^{-1}$ and 14382.0 $cm^{-1}$ agree well with the calculated value of 1.0 corresponding to transitions with $J' = J'' = 1$. However, the calculated value of $\Omega$ for transitions corresponding to $J' \neq J''$ do not agree with the observations except for that at 14393.7 $cm^{-1}$ with $\Omega = 1.5 \pm 0.1$ compared to the theoretical value of 1.5. Thus it is found that a single intermediate level approximation is not very successful in the calculation of $\Omega$ for two photon transition intensities between levels with unequal $J$ values.

The enormously large intensity of two pairs of two-photon transitions shown in figures 2b and 2c must be due to the near resonance intermediate state (figure 4). The

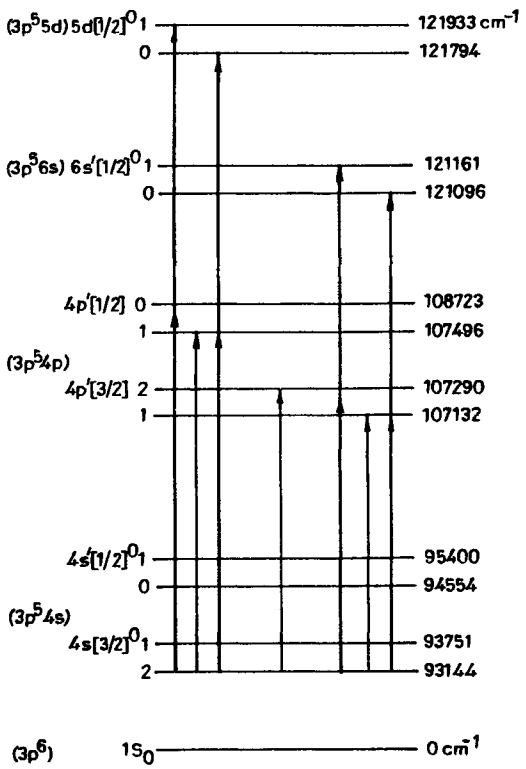


**Figure 4.** Partial energy level diagram of Ar showing (i) the $3p^5 4s$ metastable states, (ii) the strongest two-photon (heavy arrows) and one-photon (light arrows) transitions observed in figure 2 and (iii) the near resonance of $3p^5 4p$ levels as intermediate states for the two-photon transitions.

$4p'[3/2]1$ level is almost halfway between the $6s'[1/2]^\circ 1$, $6s'[1/2]^\circ 0$ upper levels and $4s[3/2]^\circ 2$ lower level involved in the two-photon transitions around $13988\,\mathrm{cm}^{-1}$. Similarly the $4p'[1/2]1$ serves as near resonant intermediate state for two-photon transitions around $14353\,\mathrm{cm}^{-1}$ (figure 4). Biraben *et al* [13] have also made parallel observations in optogalvanic spectrum of neon. The effects of linear and circular polarization on these two-photon optogalvanic signals are shown in figures 2b and 2c respectively. The one-photon lines located between the two pairs of two photon transition may be used as calibration marks for the change in relative intensities of the two-photon lines. The two-photon intensity ratio $\Omega$ (circular/linear) is found to be 1.5, 1.1, 1.3 and 0.9 for transitions to $5d[1/2]^\circ 1$, $5d[1/2]^\circ 0$, $6s'[1/2]^\circ 1$ and $6s'[1/2]^\circ 0$ upper levels respectively from the metastable $4s[3/2]^\circ 2$ level. This observation does not follow the polarization behaviour found for other two-photon transitions with unequal $J$ for upper and lower states (see preceding paragraph). The near resonance of the intermediate states and the important role of collision induced ionization [14] in the generation of optogalvanic signals may be responsible for unusual polarization characteristics of these transitions.

## 5. Conclusion

One-photon transitions exhibit a composite temporal profile with both negative and positive voltage signal whereas the two-photon transition profiles have negative voltage signal only. Linear and circular polarization studies have been carried out to distinguish different types of two-photon transitions.

A near resonant observation has been made for the first time where intermediate level in the two-photon transition happens to be a real level. This gives rise to intensity changes in the circular and linear polarizations as compared to two-photon transitions with nonresonant intermediate levels.

## Acknowledgements

Experimental work was carried out in Rutgers University, USA, while (TK) and (SNT) were visiting scientists. The authors are thankful to Prof. J Philis and Dr D Guo for many suggestions to improve the manuscript. They gratefully acknowledge financial support from the Petroleum Research Fund administered by the American Chemical Society and National Science Foundation.

## Reference

[1] M-C Su, S R Oritz and D L Monts, *Opt. Commun.* **61**, 257 (1987)
[2] G A Bickel and K K Innes, *Appl. Opt.* **24**, 3620 (1985)
[3] S N Thakur and K Narayanan, *Opt. Commun.* **94**, 59 (1992)
[4] J R Nestor, *Appl. Opt.* **21**, 4154 (1982)
[5] M H Bergemann and R J Saykally, *Opt. Commun.* **40**, 277 (1982)
[6] B R Reddy, P Venkateswarlu and M C George, *Opt. Commun.* **75**, 267 (1990)
[7] D L Monts and M-C Su, *Appl. Spectrosc.* **44**, 641 (1990)
[8] G Racah, *Phys. Rev.* **61**, 537 (1942)

[9] C E Moore, *Atomic energy levels*, NSRDS-NBS-35 (USA) **I**, 211 (1971)
[10] J E Lawler, *Phys. Rev.* **A22**, 1025 (1980)
[11] R Shuker, A Ben-Amar and G Erez, *J. Phys (Paris)* **44**, C7–35 (1983)
[12] G Grynberg, F Biraben, E Giacobino and B Cagnac, *J. Phys. (Paris)* **38**, 629 (1977)
[13] F Biraben, E Giacobino and G Grynberg, *Phys. Rev* **A12**, 2444 (1975)
[14] P R Berman, *Phys. Rev.* **A13**, 2191 (1976)